Quantifying Transport Between the Tropical and Mid-Latitude Lower Stratosphere

C. M. Volk,* J. W. Elkins, D. W. Fahey, R. J. Salawitch,
G. S. Dutton, J. M. Gilligan,† M. H. Proffitt, M. Loewenstein,
J. R. Podolske, K. Minschwaner, J. J. Margitan, K. R. Chan

Airborne in situ observations of molecules with a wide range of lifetimes (methane, nitrous oxide, reactive nitrogen, ozone, chlorinated halocarbons, and halon-1211), used in a tropical tracer model, show that mid-latitude air is entrained into the tropical lower stratosphere within about 13.5 months; transport is faster in the reverse direction. Because exchange with the tropics is slower than global photochemical models generally assume, ozone at mid-latitudes appears to be more sensitive to elevated levels of industrial chlorine than is currently predicted. Nevertheless, about 45 percent of air in the tropical ascent region at 21 kilometers is of mid-latitude origin, implying that emissions from supersonic aircraft could reach the middle stratosphere.

Tropospheric air enters the stratosphere predominantly at the tropical tropopause and is then dispersed upward and toward the poles. In the tropics, stratospheric air is lofted most efficiently, and photochemistry acts fastest to produce ozone and to convert anthropogenic source gases into reactive compounds that destroy ozone. Exchange of air between the tropics and the mid-latitudes is a fundamental component of global stratospheric transport. Because of the profound impact of transport on the distribution of long-lived stratospheric constituents, their reactive products, and ozone, models of atmospheric chemistry and transport must accurately represent exchange between tropical and mid-latitude air to provide realistic predictions of perturbations of the ozone layer. Particularly in the lower stratosphere at mid-latitudes, where observed reductions of ozone exceed model predictions (1),

C. M. Volk, G. S. Dutton, and J. M. Gilligan are with the Climate Monitoring and Diagnostics Laboratory (CMDL), National Oceanic and Atmospheric Administration (NOAA), Boulder, CO 80303, and the Cooperative Institute for Research in Environmental Sciences (CIRES), University of Colorado, Boulder, CO 80309, USA. J. W. Elkins is with NOAA/CMDL, Boulder, CO 80303, USA. D. W. Fahey is with the NOAA Aeronomy Laboratory, Boulder, CO 80303, USA. R. J. Salawitch and J. J. Margitan are with the Jet Propulsion Laboratory, California Institute of Technology, Pasadena, CA 91109, USA. M. H. Proffitt is with the NOAA Aeronomy Laboratory, Boulder, CO 80303, and CIRES, University of Colorado, Boulder, CO 80309, USA. M. Loewenstein, J. R. Podolske, and K. R. Chan are with the NASA Ames Research Center, Moffett Field, CA 94035, USA. K. Minschwaner is with the Department of Physics, New Mexico Institute of Mining and Technology, Socorro, NM 87801, USA.

*To whom correspondence should be addressed.
†Present address: Department of Physics, Vanderbilt University, Nashville, TN 37235, USA.

concentrations of ozone and related species are sensitive to transport of air from the tropics (2). Poleward transport from the tropics also disperses sulfate aerosols (3) that provide sites for heterogeneous chemistry, leading to reductions in mid-latitude ozone associated with elevated levels of chlorine and bromine (4). Recent work suggests a source for these aerosols near the tropical tropopause (5), and major volcanic eruptions provide a large intermittent source (6). Finally, the rate of mixing of mid-latitude air into the tropics is a key uncertainty in assessment of the impact of a proposed supersonic aircraft fleet on stratospheric ozone (7).

We present in situ tracer measurements from the lower stratosphere and use them in conjunction with a tropical tracer model to quantify transport into and out of the tropics in the altitude range 16 to 21 km. Most global photochemical models represent stratospheric transport in two dimensions as rapid meridional mixing superimposed on a zonal-mean circulation with ascent of air in the tropics and descent at mid- and high latitudes (8). Typically, these models extend into the tropics the region where planetary waves break to rapidly mix air (9). In this case, abundances of trace constituents with local photochemical lifetimes longer than ~1 year assume common global distributions and are thus uniquely correlated with each other throughout the stratosphere (10, 11). Mixing ratios of some long-lived constituents, however, exhibit different relations in the tropics than at mid- and high latitudes (12, 13), which suggests that the region of rapid mixing does not penetrate into the tropics. This

conclusion is consistent with satellite observations showing sharp meridional gradients in aerosol and tracer concentrations across the subtropics (6, 14) and a nearly unattenuated seasonal variation of tropical water vapor (15).

The question remains of how effectively the tropical stratosphere is isolated (16). Although model calculations based on meteorological winds have been used to quantify transport out of the tropics (17, 18), their value in assessing exchange in the reverse direction appears to be severely limited by the quality of tropical wind data (18). Tropical abundances of long-lived tracers, however, are sensitive to horizontal mixing (19) and indicate substantial entrainment of mid-latitude air into the tropics (20). Our derivation of transport rates relies on simultaneous observations of a suite of tracers with contrasting sources and sinks, representing photochemical lifetimes that span more than two orders of magnitude.

Observations. Our measurements were obtained simultaneously from instruments on board the NASA ER-2 aircraft from March through November 1994 (21). A new instrument, the airborne chromatograph for atmospheric trace species (ACATS-IV), measured CFC-11 (CCl_3F), CFC-12 (CCl_2F_2), CFC-113 ($CClF_2CCl_2F$), CCl_4, CH_3CCl_3, halon-1211 ($CBrClF_2$), and CH_4 once every 3 min with instrumental uncertainties generally less than 3% (22). Three other instruments measured N_2O, NO_y (reactive nitrogen), and O_3 once every second (23). We used mid-latitude data from 31 flights obtained at altitudes up to 21 km between 35° and 55° in both hemispheres during fall, winter, and spring. Tropical air was sampled on four flights each in late March–early April and in late October. We defined tropical air as the region equatorward of the sharp meridional gradient in the NO_y/O_3 ratio observed in the subtropics (13, 24).

Tropical tracer model. As an air parcel rises from the tropical tropopause, the mixing ratio of a tracer is governed by production and loss resulting from both local photochemistry and entrainment of extratropical air. Entrainment is associated with synoptic and planetary scale wave activity on quasi-horizontal isentropic surfaces (25). If we assume that the net effect of these events at a given altitude is represented by isentropic mixing with air of a mean mid-latitude mixing ratio and that the tropics are horizontally homogeneous, the long-term vertical evolution of a tropical tracer is given by

$$\frac{\partial \chi}{\partial \theta} Q = P - \frac{\chi}{\tau} - \gamma\chi - \frac{\chi - \chi_{mid}}{\tau_{in}} \quad (1)$$

where χ and χ_{mid} are the mean tropical and mid-latitude mixing ratios; θ is potential temperature used as a vertical coordinate (26); t is time; $Q = d\theta/dt$ is the net diabatic heating rate, equivalent to vertical ascent rate (27); P is the photochemical production rate; τ is the lifetime for photochemical loss; $\gamma = (\partial\chi/\partial t)/\chi$ is the long-term growth rate; and τ_{in} is a time scale for import of mid-latitude air. The inverse of τ_{in} is the entrainment rate into the tropics; that is, the fraction of air in a tropical air volume (at a fixed altitude) imported from mid-latitudes per unit time interval. In principle, if chemical production, loss, growth, and the ascent rate are all known as functions of θ, the entrainment time τ_{in} can be determined from observations of tracer mixing ratios in the tropics and mid-latitudes.

We obtained tropical ascent rates, Q, from two independent studies based on radiative transfer calculations and global meteorological and chemical data (28, 29). O_3 and NO_y have photochemical sources and small photochemical sinks in the lower tropical stratosphere, whereas all other species we considered have only photochemical sinks, predominantly photolysis in the ultraviolet and reaction with $O(^1D)$ (whereby NO_y is produced from N_2O) or, in the case of CH_4, reaction with OH and Cl. We calculated diurnally averaged photolysis rates with a radiative transfer model that includes Rayleigh and aerosol scattering (30). Concentrations of OH, $O(^1D)$, Cl, and

HO_2 (a minor sink for O_3) were calculated with a photochemical model constrained by ER-2 observations (31). Reaction rates and absorption cross-sections from the NASA–Jet Propulsion Laboratory compendium (32) were used. Long-term growth rates (γ) were derived from observed tropospheric trends during 1993–1994 (33).

Vertical profiles. The degree of isolation of the tropical ascent region can be estimated by comparison of vertical profiles of tracer mixing ratios observed in the tropics to profiles calculated with the assumption of unmixed ascent (unmixed profiles); that is, solutions to Eq. 1 with $\tau_{in} = \infty$ (34) (Fig. 1). Observed profiles of the longer lived species N_2O and CFC-12, and also of CH_4 and NO_y (35), deviate noticeably from unmixed profiles, indicating mixing with photochemically aged mid-latitude air (36). However, for CFC-113, CFC-11, and the shorter lived species CH_3CCl_3, CCl_4, and halon-1211 (35), with lifetimes at 19 km of ~3.1, 2.4, and 1.1 years, respectively, observed profiles fall within the uncertainty range of values calculated for unmixed ascent.

These results can be understood in terms of the relative influence of photochemistry and isentropic mixing on the evolution of the tracer mixing ratio profiles. For the longest lived species, photochemistry is so slow that profiles are essentially determined by ascent and mixing. For CFC-11 and other shorter lived species, photochemical loss occurs rapidly enough to dominate loss by mixing, and

hence the vertical profile is controlled primarily by ascent and local photochemistry. Tropical profiles of O_3 can similarly be explained largely by ascent and local photochemical production (occurring on a short time scale of ~3.5 months at 19 km) (19, 37). An estimate of the rate of entrainment of mid-latitude air can readily be obtained from the comparison in Fig. 1: The decline with altitude of the CFC-113 mixing ratio due to chemistry alone (unmixed profile) is comparable to the additional decline induced by mixing (observed profile), which implies that chemistry (χ/τ) and mixing $[(\chi - \chi_{mid})/\tau_{in}]$ are of approximately the same magnitude. Hence, $\tau_{in} \approx \tau (\chi - \chi_{mid})/\chi$, yielding an entrainment time of a few years.

Tracer correlations. Equation 1 can in principle be used to derive τ_{in} (38), but as shown above, no information about the rate of mixing is contained in observed vertical profiles of species that are shorter lived than CFC-113. Another difficulty in using Eq. 1 is its dependence on Q, which, because of its small value and seasonal and interannual variability, is considered highly uncertain for the tropical lower stratosphere (28, 29). Both deficiencies are avoided by analysis of correlations of tracer mixing ratios. Considering Eq. 1 for the mixing ratios of two tracers X and Y yields

$$\frac{\partial Y}{\partial X} = \frac{P_y - (\tau_y^{-1} + \gamma_y)Y - \tau_{in}^{-1}(Y - Y_{mid})}{P_x - (\tau_x^{-1} + \gamma_x)X - \tau_{in}^{-1}(X - X_{mid})}$$

(2)

which shows that the functional form of the tropical correlation $Y(X)$ depends only on photochemical production and loss rates, growth rates, the mid-latitude profiles, and the entrainment time. Furthermore, correlation diagrams eliminate much of the scatter attributed to atmospheric fluctuations, because spatial and temporal variations for long-lived stratospheric tracers are correlated (39). Therefore, correlations provide a more reliable measure of atmospheric transport than do vertical mixing ratio profiles.

Differences in the slopes of correlations observed at mid-latitudes and in the tropics provide a direct measure of exchange between the two regions. If isentropic mixing is fast as compared with photochemistry for two tracers throughout the mid-latitudes and the tropics, one tight correlation will exist for all latitudes, with a shape determined by the global photochemical sources and sinks of both species (11). If mixing into the tropics is slow as compared with photochemistry for both species, the tropical mixing ratios will be influenced solely by local (tropical) photochemical sources and sinks. Two species with sufficiently different spatial distributions of sources and sinks will then exhibit a correlation in the
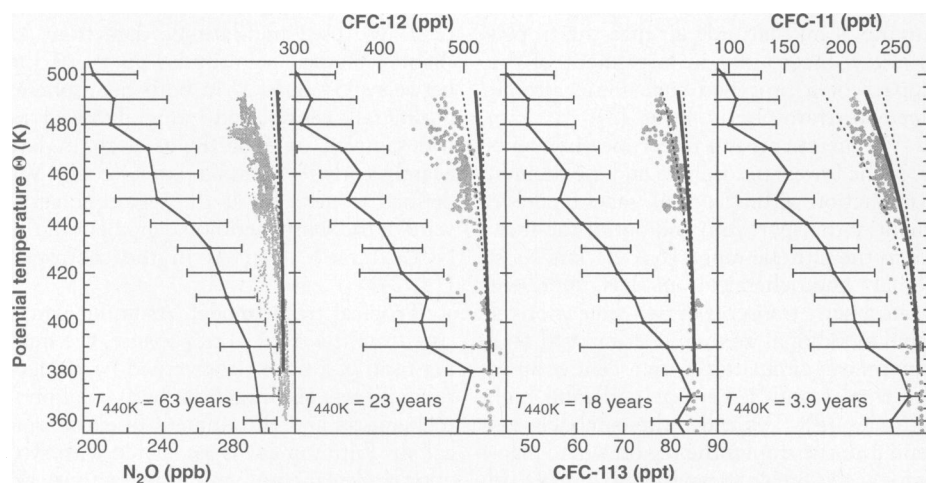

Fig. 1. Vertical profiles of mixing ratios of several long-lived trace species in the tropics (gray dots) and mid-latitudes (black squares with error bars). For the mid-latitudes, the data were binned into 10 K increments of potential temperature (θ); the profiles shown represent the bin averages and the error bars represent the standard deviation within each bin. Solid lines are calculated tropical profiles for unmixed ascent ($\tau_{in} = \infty$) from $\theta = 380$ K (the approximate mean tropopause height for the tropical observations). Calculated profiles are shown for ascent rates Q from (28); profiles based on ascent rates from (29) are similar to the ones shown. Dashed lines represent an uncertainty range in the calculated profiles induced by a 50% uncertainty in Q. Also indicated is the effective lifetime T (49) at $\theta = 440$ K (~19 km altitude) for each of the species. Species (35) that are shorter lived than CFC-11 behave similarly to CFC-11; that is, their tropical profiles agree with the unmixed profiles, within the limits of uncertainty. In particular, the observed O_3 profile closely matches the calculated unmixed O_3 profile. Mixing ratios are shown in parts per billion (ppb) or parts per trillion (ppt) by dry mole fraction.

tropics with a slope that is different from that at mid-latitudes (16). Finally, if mixing is slow as compared with photochemistry for only one of the two species, the difference of the correlation slope in the tropics from the slope at mid-latitudes will be sensitive to the magnitude of mixing into the tropics.

As an example, for a given mixing ratio of N_2O, the shorter lived species show lower abundances in the tropics than at mid-latitudes because their loss processes are larger near ~20 km (Fig. 2). N_2O is not destroyed until the air reaches higher altitudes (before descent back to low altitude in mid-latitude regions). Because the abundance of N_2O in the tropics is sensitive to isentropic mixing, however, the tropical correlations do not match the correlations calculated with the assumption of unmixed ascent (unmixed correlations). The separation of tropical and mid-latitude correlations is most pronounced for halon-1211 (the shortest lived tracer) and diminishes for species with increasing photochemical lifetime, as local chemistry becomes less important relative to mixing in determining the tropical abundance of each tracer. Tropical correlations of the longer lived species (CFC-113, CFC-12, CH_4, and NO_y) with N_2O (35) exhibit the same slope as do mid-latitude correlations, which implies that, over the altitude range considered, the local photochemical time scales of these compounds are long as compared with mixing time scales. Quantification of mixing rates with the use of these longer lived species requires correlations with a molecule whose evolution is dominated by local photochemistry, such as O_3 (Fig. 3). In such a comparison, the slope of the tropical correlation is most sensitive to mixing for the longest lived species. Tropical correlations of the shorter lived species (CFC-11, CH_3CCl_3, CCl_4, and halon-1211) with O_3 (35) are similar to the unmixed correlations and thus do not provide quantitative information about mixing.

Rates of transport. The correlation diagrams in Figs. 2 and 3 can be used to derive rates of transport between the tropics and mid-latitudes during the measurement period. We integrate Eq. 2, constrained by mixing ratios for mid-latitudes from our observations, computed photochemical sources and sinks (30, 31), and observed long-term growth rates (33) to calculate the tropical correlation Y(X) of two species, treating the entrainment time τ_{in} as a free parameter (40). Direct inversion of Eq. 2 to yield a value of τ_{in} as a function of altitude is not practical because the tropical tracer measurements exhibit too much variability to define the slope of the tropical correlation ($\partial Y / \partial$) diagram at each altitude (41). Initially, we assume a value for τ_{in} independent

of altitude. For each pair of tracers displayed in Figs. 2 and 3, we determined the value of τ_{in} giving best agreement with the observations by an iterative least-squares fit of the calculated correlation (shown in Figs. 2 and 3) to the observed tropical correlation. Analysis of each correlation diagram (Fig. 4) yields a geometric mean (weighted by the individual uncertainties) for τ_{in} of 13.5 months, with an uncertainty of ~20% (42). Individual determinations of τ_{in} from each pair of tracers agree with this mean value. This result is indicative of a vertically averaged entrainment rate into the tropics of 7% per month ($1/\tau_{in}$) over the altitude range 16 to 21 km during 1994. The average entrainment time of 13.5 months is longer than the time scale for isentropic mixing at mid-latitudes of less than 3 months (43), which confirms that mixing into the tropics is slow compared with mixing within mid-latitudes.

The data do not provide information on the dependence of τ_{in} with height. Following the inversion procedure outlined above, but allowing τ_{in} to vary linearly with altitude, we found no evidence for either a significant increase or decrease of the entrainment time with altitude. This result is also evident from the good fits to the observed correlations obtained when values of τ_{in} independent of altitude are used (Figs. 2

and 3). Conceptually, the altitude dependence of τ_{in} is implicit in the detailed shape of the tropical correlation. The tropical correlations displayed in Figs. 2 and 3, because of their variability and limited range, do not reveal details about their shape much beyond their average slope; the altitude dependence of τ_{in} therefore cannot be resolved. Another complication is posed by the convolution of space and time not explicit in the time-averaged formulation of Eq. 1: Because tropical air at any given altitude carries the integrated signature of mid-latitude intrusions from the time it crossed the tropopause, the detailed shape of the tropical correlation at a given time is determined not solely by the altitude dependence of isentropic mixing but also by the time history of mixing, photochemistry, and mid-latitude abundances. Consequently, tropical and mid-latitude measurements from many different seasons are needed to unravel both the temporal and height dependence of τ_{in}; neither can be determined from our tropical observations covering only two seasons. However, an average over several seasons is implicit in our vertically averaged determination of τ_{in}, because the observations cover an altitude interval that a rising air parcel crosses during the course of several seasons (44).

Fig. 2. Correlations of mixing ratios for the shorter lived species versus N_2O in the tropics (dark gray dots) and at mid-latitudes (light gray dots). Thin solid lines represent mean mid-latitude correlations used in the calculations (40) and were obtained from quadratic fits to the correlations. Thick dotted lines are calculated correlations for the unmixed case ($\tau_{in} = \infty$). Thick solid lines are calculated tropical correlations for a constant entrainment time τ_{in} that yielded the best agreement (in a least-squares sense) with the observed tropical correlations. All fits are shown over a N_2O range that corresponds to the potential temperature range $\theta = 380$ K to $\theta = 492$ K (the stratospheric θ-range of the tropical data). Also indicated is the effective lifetime T (49) at $\theta = 440$ K for each of the species.
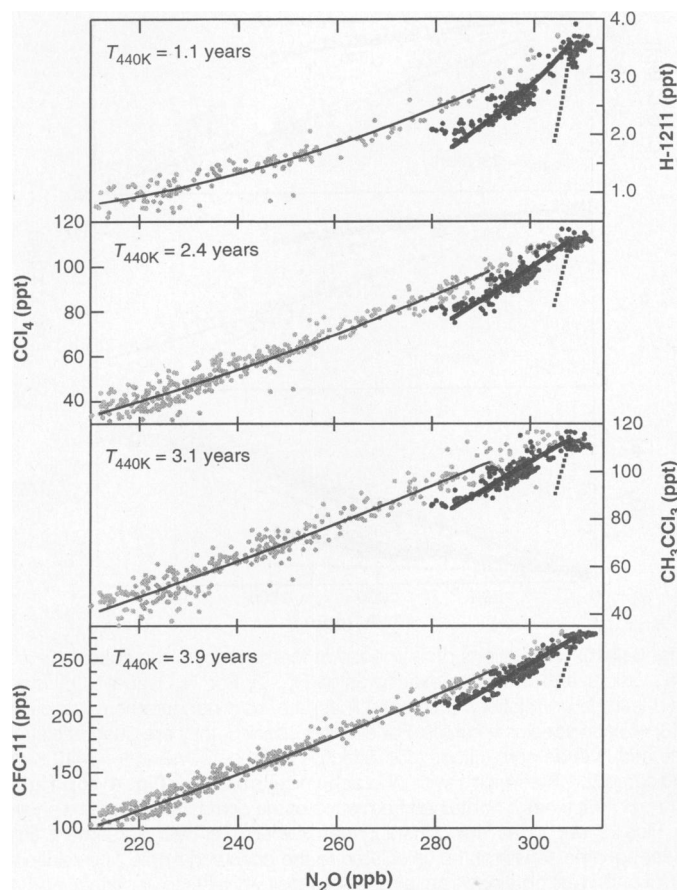
Equatorward entrainment of air into the tropics is not necessarily balanced by poleward detrainment from the tropics. A rough estimate for the rate of detrainment can be made with the assumption of a steady mass balance across the tropical–mid-latitude boundary and the rate of entrainment determined above. In the annual mean, the net mass flux out of the tropics (detrainment minus entrainment) must be balanced by the mean mass divergence within the tropics (determined from the mean ascent rate)

$$\frac{\rho}{\tau_{out}} - \frac{\rho}{\tau_{in}} = -\frac{\partial}{\partial z}(\rho w) \qquad (3)$$

where τ_{out} is a time scale for export of air, ρ is the air density, z is altitude, and w is the mean vertical velocity. The inverse of τ_{out} is the mean detrainment rate; that is, the fraction of air in a tropical air volume (at a fixed altitude) exported to mid-latitudes per unit time. Detrainment rates computed from Eq. 3 for our estimate of τ_{in} (13.5 months) and ascent velocities averaged over 24 months (28, 29) show that, over much of the altitude range considered, more air is exported from the tropics than is imported (Fig. 5A). The derived detrainment rates and their vertical profiles are dominated by the mass divergence term and are not very sensitive to τ_{in} (45). These rates should be indicative of the total trans-

port from the tropics to both hemispheres averaged over 2 years. The corresponding detrainment time (τ_{out}) of less than ~6 months below 19 km is consistent with observations of rapid propagation of the seasonal cycles of CO_2 and H_2O from the tropics to mid-latitudes in the lowest several kilometers of the stratosphere (43, 46). These observations also show that the seasonal signals of CO_2 and H_2O fade quickly at mid-latitudes (but not in the tropics) above 19 km, indicating slower detrainment from the tropics at these altitudes. This morphology of decreasing detrainment at higher altitudes is also supported by studies of aerosol dispersal from the tropical reser-
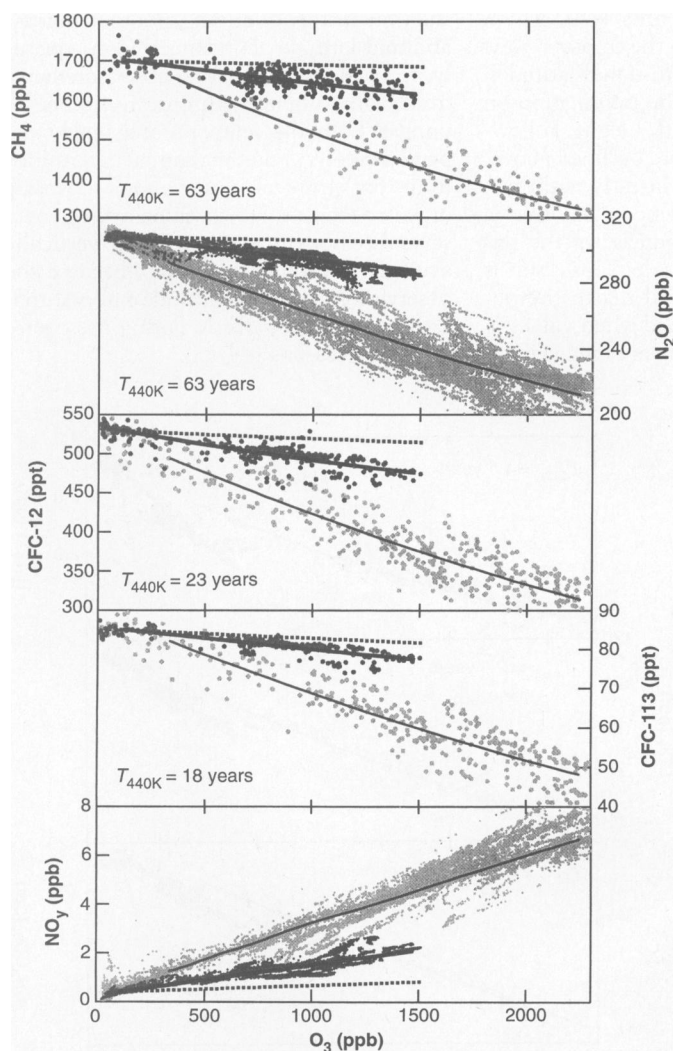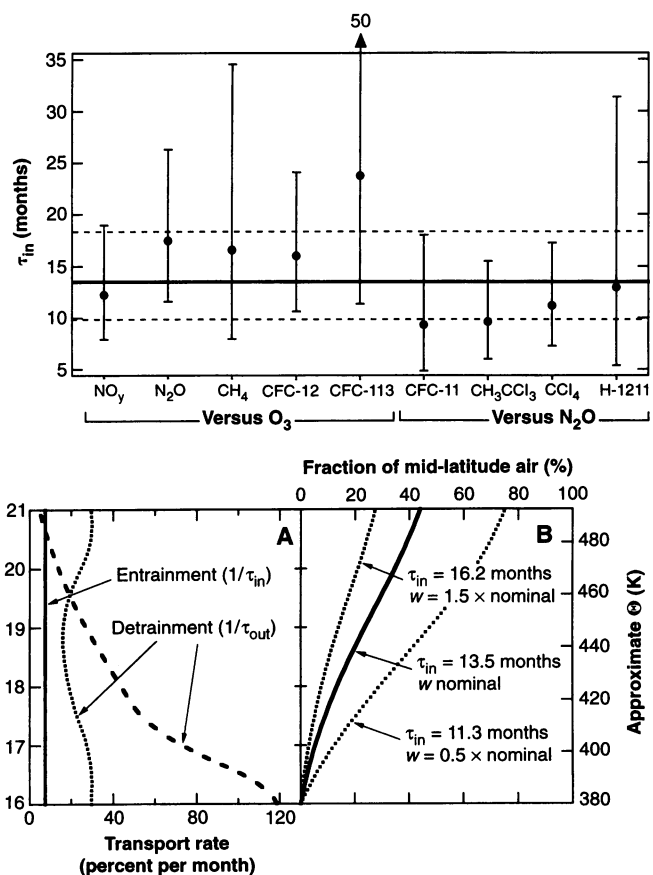

the inputs used in the calculation (including uncertainties of fits and initial values) under the assumption that individual inputs are independent of each other. The error bars are symmetric on a logarithmic scale (42). The thick solid line is the weighted geometric mean (13.5 months); its uncertainty, expressed as an uncertainty factor, is 1.2. Dashed lines reflect the range of one standard deviation.   **Fig. 5 (bottom right).** (**A**) Entrainment rate (solid line) into and detrainment rates out of the tropics versus altitude, expressed as the fraction of air within a tropical air volume (at a fixed altitude) entrained and detrained per month. Results are for τ_{in} = 13.5 months and for ascent rates from (28) (dashed line) and (29) (dotted line). The disagreement between detrainment rates based on (28) and (29) reflects differences in the vertical profiles of the ascent rates (45). (**B**) Fraction of mid-latitude air within the tropics versus altitude for nominal (solid line) and extreme (dotted lines) values of τ_{in} and ascent rates w from (28) as indicated. The corresponding result for ascent rates from (29) agrees to within ~5%. To facilitate comparison with Fig. 1, the approximate potential temperature [valid for both (A) and (B)] is given on the right axis.

Fig. 3 (left). Correlations of mixing ratios for the longer lived species versus O_3. Colors and lines are exactly as in Fig. 2. For N_2O and NO_y, mean mid-latitude correlations (thin solid lines) are from nonparametric loess fits (48) of each species versus θ. For all other species, they are quadratic fits to the mid-latitude correlations (40). Effective lifetimes T (49) at θ = 440 K are indicated for the species with photochemical sinks.   **Fig. 4 (top right).** Entrainment times τ_{in} obtained from each of the correlation diagrams shown in Figs. 2 and 3 as the constant that yielded the best agreement (in a least-squares sense) of the calculated to the observed tropical correlations. Error bars were obtained from a series of sensitivity tests to uncertainties of all

voir (*3*, *6*) and by transport analyses based on meteorological winds (*17*, *18*). Recent analysis (*18*) has shown that transport rates from the tropics to the northern hemisphere are about 8 to 10% (of tropical mass) per month at 18.5 and 21 km, which is in reasonable agreement with our result of a total detrainment rate to both hemispheres of 5 to 35% in this altitude range.

As shown in Fig. 5B, ~45% of air of extratropical origin accumulates in a tropical air parcel during its ~8-month ascent from the tropopause to 21 km. This estimate assumes an entrainment time of 13.5 months and rapid homogenization of newly entrained air in the tropics. The result is insensitive to the altitude dependence of the entrainment rate but depends directly on the magnitude of the ascent velocity and thus has a large uncertainty (Fig. 5B). Regardless, entrainment of mid-latitude air into the tropical ascent region of the lower stratosphere is significant.

Implications. Our measurements and analysis demonstrate that tropical air is relatively isolated from mid-latitudes, where isentropic mixing occurs more rapidly. However, because the time scale for tropical ascent is comparable to the entrainment time scale, there is considerable accumulation of extratropical air in the inner tropics. Our observations suggest that nearly half the air in the tropical ascent region at 21 km has been transported from mid-latitudes. This implies that a significant fraction of NO_x (= NO + NO_2) and other effluents emitted from supersonic aircraft at mid-latitudes between 16 and 23 km will probably reach the middle and upper stratosphere, where enhancements in NO_x are expected to lead to reductions in ozone (*7*). Although estimation of the effects of human activity on ozone remains a task for multidimensional models of atmospheric transport and chemistry, our determination of the rates of transport and the fraction of mid-latitude air within the tropical ascent region constitutes an important test for the accuracy of such models. Most current two-dimensional models do not reproduce steep meridional tracer gradients in the subtropics, such as that observed in the NO_y/O_3 ratio (*8*, *13*), which suggests that they generally overestimate the magnitude of mixing between the tropics and mid-latitudes (*7*). Restricting exchange with the tropical production regions of ozone would tend to enhance the relative influence of chemical sinks on ozone concentrations at mid-latitudes. More isolated tropical ascent would also imply more direct transport of tropospheric source gases to their tropical sink regions, accelerating the overall stratospheric release of inorganic halogens. Ozone at mid-latitudes might thus be ex-

pected to be more sensitive to chemical loss induced by elevated levels of industrial halocarbons and volcanic aerosols than many models currently predict. Tests with a particular two-dimensional model indeed show that greater reductions of mid-latitude ozone are calculated, improving agreement with observed trends, if mixing parameters are modified to simulate restricted exchange across the tropics (*47*). Realistic representation of dynamic coupling between the tropical source and mid-latitude sink regions of ozone may thus hold the key to understanding and reliable prediction of the response of the stratospheric ozone layer to a variety of anthropogenic as well as natural perturbations.

REFERENCES AND NOTES

1. Global Ozone Research and Monitoring Project—Report 37 (World Meteorological Organization, Geneva, Switzerland, 1995).
2. M. K. W. Ko, N. D. Sze, D. K. Weisenstein, *J. Geophys. Res.* **94**, 9889 (1989).
3. C. R. Trepte, R. E. Veiga, M. P. McCormick, *ibid.* **98**, 18563 (1993); W. B. Grant *et al.*, *ibid.* **101**, 3973 (1996).
4. G. Brasseur and C. Granier, *Science* **257**, 1239 (1992); D. W. Fahey *et al.*, *Nature* **363**, 509 (1993); J. C. Wilson *et al.*, *Science* **261**, 1140 (1993); P. O. Wennberg *et al.*, *ibid.* **266**, 398 (1994).
5. C. A. Brock, P. Hamill, J. C. Wilson, H. H. Jonsson, K. R. Chan, *Science* **270**, 1650 (1995).
6. C. R. Trepte and M. H. Hitchman, *Nature* **355**, 626 (1992); M. H. Hitchman, M. McKay, C. R. Trepte, *J. Geophys. Res.* **99**, 20689 (1994).
7. R. S. Stolarski *et al.*, *NASA Ref. Publ. 1381* (1995).
8. M. J. Prather and E. E. Remsberg, Eds., *NASA Ref. Publ. 1292* (1993).
9. M. E. McIntyre and T. N. Palmer, *Nature* **305**, 593 (1983).
10. J. R. Holton, *J. Geophys. Res.* **91**, 2681 (1986); J. D. Mahlman, H. Levy II, W. J. Moxim, *ibid.*, p. 2687.
11. R. A. Plumb and M. K. W. Ko, *ibid.* **97**, 10145 (1992).
12. P. D. Goldan, W. C. Kuster, D. L. Albritton, A. L. Schmeltekopf, *ibid.* **85**, 413 (1980); M. H. Proffitt, D. W. Fahey, K. K. Kelly, A. F. Tuck, *Nature* **342**, 233 (1989).
13. D. M. Murphy *et al.*, *J. Geophys. Res.* **98**, 8751 (1993); D. W. Fahey *et al.*, *Geophys. Res. Lett.*, in press.
14. W. J. Randel *et al.*, *Nature* **365**, 533 (1993).
15. P. W. Mote *et al.*, *J. Geophys. Res.* **101**, 3989 (1996).
16. R. A. Plumb, *ibid.*, p. 3957.
17. R. Rood, A. Douglass, C. Weaver, *Geophys. Res. Lett.* **19**, 805 (1992); P. Chen, J. R. Holton, A. O'Neill, R. Swinbank, *J. Atmos. Sci.* **51**, 3006 (1994).
18. D. W. Waugh, *J. Geophys. Res.* **101**, 4007 (1996).
19. L. M. Avallone and M. J. Prather, *ibid.*, p. 1457.
20. K. Minschwaner *et al.*, *ibid.*, p. 9433.
21. During the flight campaign [the Airborne Southern Hemisphere Ozone Experiment/Measurements for Assessing the Effects of Stratospheric Aircraft (ASHOE/MAESA)] the ER-2 sampled air from 60°N to 70°S up to 21 km.
22. J. W. Elkins *et al.*, *Geophys. Res. Lett.*, **23**, 347 (1996).
23. J. R. Podolske and M. Loewenstein, *Appl. Opt.* **32**, 5324 (1993); D. W. Fahey *et al.*, *J. Geophys. Res.* **94**, 11299 (1989); M. H. Proffitt and J. McLaughlin, *Rev. Sci. Instrum.* **54**, 1719 (1983). Data used here are averaged over 10-s intervals.
24. As shown in (*13*), the NO_y/O_3 ratio is markedly lower in the tropics than anywhere else in the stratosphere. Hence, NO_y/O_3 is a good tracer for tropical air. The latitudinal range of the selected tropical data varied from flight to flight and between the two seasons

sampled. The tropical observations span 10°N to 26°S in late March–early April 1994 and 19°N to 14°S in late October 1994; most of the data fall within 12° of the equator.
25. As used here, "exchange" between the tropics and mid-latitudes and related terms therefore refer to isentropic (that is, adiabatic) processes.
26. Potential temperature is the temperature an air parcel would attain if it were adiabatically compressed or expanded from the local pressure to 10^5 Pa. Potential temperature is a conserved quantity for isentropic air motions and is a monotonically increasing function of altitude in the stratosphere. Its use as a vertical coordinate in Eq. 1 is convenient because isentropic mixing occurs horizontally in this coordinate system. The tropical profile of potential temperature versus pressure altitude adopted in the model is based on temperature data from the U.K. Meteorological Office data assimilation system. The data were averaged from 10°N to 10°S over a 24-month period (November 1993 to October 1994).
27. If potential temperature θ is used as a vertical coordinate, a vertical displacement implies diabatic gain or loss of heat.
28. K. H. Rosenlof, *J. Geophys. Res.* **100**, 5173 (1995). Ascent rates were averaged from 10°N to 10°S and over a 24-month period (September 1992 to August 1994). The uncertainty of these calculations in the lower stratosphere is estimated as ~50% above 18 km and even more just above the tropopause.
29. J. Eluszkiewicz *et al.*, *J. Atmos. Sci.* **53**, 217, 1996. Results were averaged as described above (*28*). Uncertainties are estimated as ~50%. The averaged tropical heating rates agree with those obtained from (*28*) within the estimated uncertainties.
30. K. Minschwaner, R. J. Salawitch, M. B. McElroy, *J. Geophys. Res.* **98**, 10543 (1993). The model is constrained by vertical profiles for O_3 from a climatology (based on satellite, sonde, and in situ measurements) that was scaled to match total column measurements from the Total Ozone Mapping Spectrometer and by vertical profiles for temperature and aerosol extinction from the National Meteorological Center and the Stratospheric Aerosol and Gas Experiment II, respectively. We averaged photolysis rates calculated for winter, summer, and the equinox, and for latitudes from 10°N to 10°S. Uncertainties in the photolysis rates are ~20% for most species.
31. R. J. Salawitch *et al.*, *Geophys. Res. Lett.* **21**, 2551 (1994).
32. *Chemical Kinetics and Photochemical Data for Use in Stratospheric Modeling, Evaluation No. 11*, JPL Publ. 94-26 (NASA, Jet Propulsion Laboratory, Pasadena, CA, 1994).
33. S. A. Montzka *et al.*, *Science*, in press; J. W. Elkins and E. J. Dlugokencky, unpublished data from the NOAA/CMDL global network. Methods and trend analysis are described in J. W. Elkins *et al.*, *Nature* **364**, 780 (1993); and E. J. Dlugokencky, L. P. Steele, P. M. Lang, K. A. Masarie, *J. Geophys. Res.* **99**, 17021 (1994). Only data from tropical stations were used. Although the growth rates are less than a few percent per year, they are generally of the same order as photochemical loss rates near the tropical tropopause.
34. The unmixed case corresponds to the "tropical pipe" model in (*16*).
35. C. M. Volk *et al.*, data not shown.
36. Much of the mid-latitude air in the lower stratosphere has at one time been lofted to higher altitudes in the tropics before descending in the downward branch of the stratospheric circulation cell. Because of the increasing intensity of ultraviolet radiation with altitude, this air has "photochemically aged," resulting in lower mixing ratios for the species displayed in Fig. 1 at mid-latitudes than in the tropics.
37. A. E. Dessler *et al.*, *J. Atmos. Chem.* **23**, 209 (1996).
38. This approach is pursued in (*20*).
39. D. H. Ehhalt, E. P. Röth, U. Schmidt, *J. Atmos. Chem.* **1**, 27 (1983).
40. For the integration, all observational inputs are first established as functions of potential temperature θ. Mean mid-latitude mixing ratios for N_2O, O_3, and NO_y (the species sampled at high frequency) are obtained from nonparametric loess fits (*48*) versus θ.

For the other species (where much less data is available), mean mid-latitude mixing ratios are then deduced from quadratic fits to the mid-latitude correlations versus N_2O or O_3, as shown in Figs. 2 and 3. A relation between θ and the tropical mixing ratios X (of N_2O and O_3), again from a loess fit versus θ, is then used to transform the coordinate system from θ to X. Finally, Eq. 2 is solved as a differential equation of Y in X to calculate the tropical correlation $Y(X)$. Initial (tropical tropopause) mixing ratios are obtained by averaging of all measurements taken in the upper tropical troposphere during the flight campaign.

41. The shape of τ_{in} as function of altitude determined by direct inversion of Eq. 2 depends sensitively on the choice of functional fit to the tropical data to determine $\partial Y/\partial X$ versus altitude; its geophysical meaning is therefore questionable.

42. Because uncertainties for individual determinations of τ_{in} as provided by sensitivity tests were approximately symmetric on a logarithmic rather than a linear scale, we evaluated all statistical quantities for $\log(\tau_{in})$ rather than τ_{in}. The weighted mean is thus equivalent to a weighted geometric mean and its uncertainty is best expressed as an uncertainty factor that evaluated to 1.2.

43. K. A. Boering et al., Geophys. Res. Lett. 21, 2567 (1994); E. J. Hintsa et al., ibid., p. 2559; K. A. Boering et al., ibid. 22, 2737 (1995).

44. Based on the ascent rates from (28, 29), ascent of tropical air from the tropopause to 21 km takes ~8 months. Hence, the two observational snapshots in March/April and October 1994 combine air influenced by mixing during the time span of at least a full seasonal cycle. Differences between the March/April and October tropical observations on a given potential temperature level were generally smaller than flight-to-flight variability.

45. Because of the large uncertainty in the ascent rates (28, 29), mean detrainment rates obtained by this simple argument must be considered uncertain to at least 50%. The increase above 19 km in the detrainment rate based on (29) is caused by anomalously low net heating rates at 46 hPa that are thought to be an artifact of a known low bias in Microwave Limb Sounder O_3 satellite measurements (29).

46. M. P. McCormick et al., J. Geophys. Res. 98, 4867 (1993).

47. M. K. W. Ko, personal communication. The model calculated the decadal change in the ozone column between 1980 and 1990, as well as the transient ozone change in response to increased aerosol loading after the eruption of Mount Pinatubo in June 1991. A description of the model is given in M. K. W. Ko, K. K. Tung, D. K. Weisenstein, and N. D. Sze [J. Geophys. Res. 90, 2313 (1985)]; restricted mixing was achieved by a decrease in the horizontal diffusion coefficient within the tropical lower stratosphere as described in D. K. Weisenstein, M. K. W. Ko, N. D. Sze, and J. M. Rodriguez [Geophys. Res. Lett. 23, 161 (1996)]. Restriction of mixing across the tropics also resulted in an ~20% decrease of the calculated lifetimes of tropospheric source gases.

48. W. S. Cleveland, J. Am. Stat. Assoc. 74, 829 (1979).

49. The effective lifetime is $T = 1/(\tau^{-1} + \gamma)$. T is the relevant time scale for the combined effects of local growth and photochemical loss that determine the vertical profile of the tropical abundance in the absence of mixing. Because photochemical loss is the dominant factor (above ~18 km) for the species considered here, we refer to T simply as lifetime or photochemical lifetime.

50. We thank K. H. Rosenlof and J. Eluszkiewicz for providing data for tropical ascent rates and suggestions; R. A. Plumb, M. K. W. Ko, and F. L. Moore for discussions; P. J. Fraser, L. P. Steele, M. P. Lucarelli, and S. A. Montzka for support during the field deployments in New Zealand; and our many colleagues of the 1994 ASHOE/MAESA campaign, especially the pilots of the ER-2 aircraft. Supported in part by NASA's Upper Atmospheric Research Program, the Atmospheric Effects of Stratospheric Aircraft component of the NASA High-Speed Research Program, and the Atmospheric Chemistry Project of NOAA's Climate and Global Change Program.

10 January 1996 ; accepted 17 April 1996

AAAS–Newcomb Cleveland Prize

To Be Awarded for a Report, Research Article, or an Article Published in *Science*

The AAAS–Newcomb Cleveland Prize is awarded to the author of an outstanding paper published in *Science*. The value of the prize is $5000; the winner also receives a bronze medal. The current competition period began with the 2 June 1995 issue and ends with the issue of 31 May 1996.

Reports, Research Articles, and Articles that include original research data, theories, or syntheses and are fundamental contributions to basic knowledge or technical achievements of far-reaching consequence are eligible for consideration for the prize. The paper must be a first-time publication of the author's own work. Reference to pertinent earlier work by the author may be included to give perspective.

Throughout the competition period, readers are invited to nominate papers appearing in the Reports, Research Articles, or Articles sections. Nominations must be typed, and the following information provided: the title of the paper, issue in which it was published, author's name, and a brief statement of justification for nomination. Nominations should be submitted to the AAAS–Newcomb Cleveland Prize, AAAS, Room 1044, 1200 New York Avenue, NW, Washington, DC 20005, and **must be received on or before 30 June 1996**. Final selection will rest with a panel of distinguished scientists appointed by the editor-in-chief of *Science*.

The award will be presented at the 1997 AAAS annual meeting. In cases of multiple authorship, the prize will be divided equally between or among the authors.

Science

Quantifying Transport Between the Tropical and Mid-Latitude Lower Stratosphere

C. M. Volk, J. W. Elkins, D. W. Fahey, R. J. Salawitch, G. S. Dutton, J. M. Gilligan, M. H. Proffitt, M. Loewenstein, J. R. Podolske, K. Minschwaner, J. J. Margitan and K. R. Chan

ARTICLE TOOLS	http://science.sciencemag.org/content/272/5269/1763
REFERENCES	This article cites 43 articles, 4 of which you can access for free http://science.sciencemag.org/content/272/5269/1763#BIBL
PERMISSIONS	http://www.sciencemag.org/help/reprints-and-permissions

Use of this article is subject to the Terms of Service